Hindawi
Discrete Dynamics in Nature and Society
Volume 2022, Article ID 3790548, 15 pages
https://doi.org/10.1155/2022/3790548

Research Article

Following Consistency of Energy-Saving Operation for Urban Rail Trains Based on Event Triggering Mechanism

Ruxun Xu,[1,2,3,4] Jianjun Meng,[1,2,3,4] Juhui Zhang,[1,2,3,4] Xiaoqiang Chen,[1,2,3,4] and Decang Li[1,2,3,4]

[1]*Mechatronics T&R Institute, Lanzhou Jiaotong University, Lanzhou 730070, China*
[2]*School of Mechatronic Engineering, Lanzhou Jiaotong University, Lanzhou 730070, China*
[3]*Gansu Provincial Engineering Technology Center for Informatization of Logistics & Transport Equipment, Lanzhou 730070, China*
[4]*Gansu Provincial Industry Technology Center of Logistics & Transport Equipment, Lanzhou 730070, China*

Correspondence should be addressed to Jianjun Meng; mengjj1966@163.com

Received 27 June 2022; Revised 9 November 2022; Accepted 18 November 2022; Published 8 December 2022

Academic Editor: Jesus M. Munoz-Pacheco

To reduce the traction energy consumption of urban rail trains by regenerating energy, a train traction and braking model was designed based on algebraic graph theory and train dynamics theory and the following consistency model of energy-saving operation of urban rail trains was constructed based on the conditions of the coordination coefficient and the operating condition conversion of trains. Not only to constantly update the consistency controller and save communication resources but also to optimize the energy-saving effect, the consistency algorithm of event triggering was used to search for the optimal operating conditions of trains and the energy-saving operation scheme for multiple trains was established. Taking the train diagram of a subway line in Jinan as an example, the energy-saving control scheme of four trains was solved by MATLAB simulation. The simulation results show that the model can not only ensure parking accuracy and punctuality but also energy savings effectively; that is, the proportion of the total regenerative energy used by the follower train in the actual energy consumption is increased from 3.32% to 10.76%, and the actual total energy consumption of the train is reduced by 9.23%.

1. Introduction

With the continuous expansion of the construction scale of urban rail transit, the energy consumption of urban rail trains shows a rapid growth trend. Among all kinds of energy consumption of urban rail transit systems, the proportion of traction energy consumption of trains in the total energy consumption is the most prominent. How to reduce traction energy consumption by optimizing the train operation is a common concern of operation companies and scholars [1]. Due to the short distance between urban rail transit stations, frequent braking during train operation will produce considerable regenerative energy, which can be fed back to the catenary for immediate use by other traction trains. Therefore, efficient and full utilization of renewable energy is an important way to reduce the energy consumption of urban rail transit systems [2].

At present, to improve the utilization of renewable energy, many scholars at home and abroad mainly study the optimization of train schedules and train coordinated control. The optimization of train schedules can improve the utilization rate of renewable energy and reduce actual energy consumption from the perspective of the entire system [3], mainly including optimizing the arrival and departure times, departure intervals, and interstation operation redundancy time allocation [4–6]. From the perspective of train cooperative control, some scholars have studied how to increase the heavy fall time of train traction and braking conditions through the cooperative operation process of multiple trains, so as to improve the utilization rate of renewable energy [7–10]. Although some methods mentioned in the literature [3–10] have improved the utilization rate of renewable energy, they have had some impact on the operation schedule of

urban rail trains. The train cooperative control is extended to the general agent cooperative control, and its control basis is the consistency problem, which refers to that multiple control systems update their own information by the information about themselves and leaders, so as to make a certain negotiation variable tend to be consistent [11]. The control systems communicate by the network in practical application, and because of the bandwidth and other constraints of the network itself, it brings higher challenges to multisystem cooperative control [12]. Therefore, Tabuada and other scholars proposed a new method of event-triggered communication [13]. At present, the research on event-triggered multisystem consistency has made many achievements [14–17]. Chen et al. [18] introduced an event trigger mechanism to avoid excessive consumption of communication resources. Li et al. [19] proposed an event trigger strategy to reduce the communication burden of the two channels from the device and model to the controller. Zhou and Chang [20] applied an elastic trigger mechanism to reduce the communication channel load and save network resources.

As an important consistency problem, following consistency has also attracted the attention of more and more scholars. In this kind of problem, the leader is not affected by other followers, and under the action of consistency agreement, a negotiation variable changes with the leader [21–23]. The works [11–23] have studied the application of event-triggering mechanism and consistency protocol in other fields, which provides a reference for this study.

Under the condition of not changing the train schedule [24], we studied the application of the following consistency event in the energy-saving operation of urban rail trains, introduced the event trigger mechanism into the following consistency collaborative control, took the weighted acceleration of the train as the collaborative variable, changed the secondary traction time of the follower train through the event trigger mechanism, and increased the renewable energy utilization rate of the leader train, and it not only reduced the traction energy consumption but also ensured the punctuality of train operation at each station.

2. Problem Description

Consider that the leading urban rail vehicle is the leader and the following vehicle is the follower, a multiagent system is formed. The dynamic models of the leader and follower are shown in

$$\dot{x}_0(t) = Ax_0(t), \tag{1}$$

$$\dot{x}_i(t) = Ax_i(t) + B\tau sat\left(u_i(t)\right), \tag{2}$$

where $x_0(t)$ and $x_i(t) \in R^n$ are the states of the leader and follower, respectively, $A \in R^{n\times n}$ and $B \in R^{n\times p}$ are the system matrices, $u_i(t) \in R^p$ is the control input of the follower, τ is the traction control coefficient, and $sat(\cdot)$ represents a symmetric input saturation function, as shown in

$$sat\left(u_i\right) = \begin{cases} u_{\max}, & u_i > u_{\max} \\ u_i, & \left|u_i\right| \le u_{\max} \\ -u_{\max}, & u_i < -u_{\max} \end{cases}. \tag{3}$$

According to the actual situation of urban rail transit, under the control input saturation constraint of the follower, a consistency control strategy is designed to reduce the update frequency of the controller, so as to reduce network consumption and avoid network congestion and delay the network's life. Therefore, it is assumed that the leader and follower trains are installed with an event monitor to determine the time when communication is required and the control input is updated.

The research of this paper is based on the following assumptions:

(1) The running time and dwell time of each station interval of the subway train are constant and cannot be adjusted.

(2) The operation curve of the leader train is determined by the optimal energy-saving operation scheme of the traditional single train operation, which is not variable, that is, the maximum traction force is adopted for traction under traction conditions, the maximum braking force is adopted for braking under braking condition, and the coasting condition is adopted in the middle [25]; The operating condition of the follower train is to draw to the set speed with the maximum traction force and then coasting. During this coasting, consistent coordination is accepted. According to the coordination or coasting to the last moment that can meet the operation time and distance, retraction (traction equivalent to the braking force)-coasting braking (maximum braking force) occurs.

(3) Assuming that the train is in the same power supply arm, the regenerative braking electric energy of the leader train can be used by other following trains immediately and the remaining energy can be consumed by trackside resistance. The utilization process is shown in Figure 1. In Figure 1, train 1 is in the traction condition stage and train 0 is in the braking condition stage. The regenerative energy generated by train 0 braking can be immediately utilized by train 1, which is reflected in the feasibility of path 1. In addition, when the electric energy required by train 1 during traction is less than the regenerative energy generated by train 0, the excess regenerative energy is consumed by trackside resistance, that is, path 2 is feasible; in addition, when the electric energy required by train 1 is greater than the regenerative energy generated by train 0, the regenerative energy generated by train 0 is feasible. Path 4 will not exist. At this time, the traction substation will transmit enough electric energy for

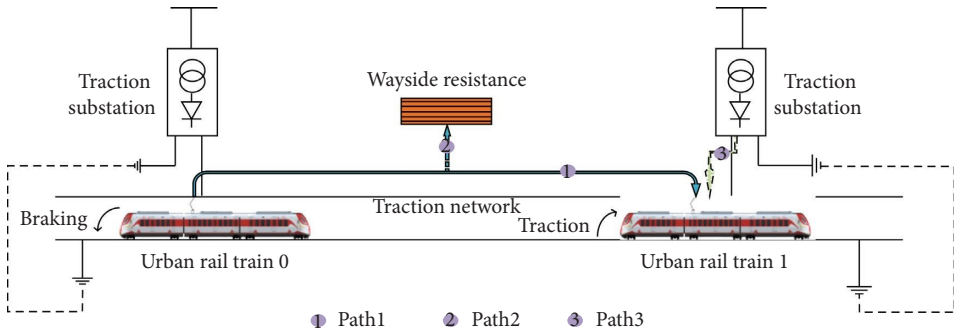

Figure 1: Schematic diagram of regenerative energy utilization process.

train 1 to ensure the normal operation of train 1, which is reflected in the feasibility of path 3.

(4) To ensure the accuracy of train operating time, it is assumed that the train will not be affected by coordinated control under the outbound traction condition and inbound braking condition, that is, the maximum traction force and maximum braking force will remain unchanged.

(5) Due to the influence of the urban rail transit operating environment and operation requirements, the maximum traction acceleration of the train is set as $a_{t\max}$, the maximum braking acceleration is set as $a_{b\max}$, and the maximum speed limit is set as $v_{\max}$,

(6) The consistency of multitrain energy-saving cooperative operations is studied. The train is regarded as a particle, and the operation conditions such as ramps and tunnels of the line are not considered for the time being.

3. Train Operation Model

3.1. Force Analysis. The train is mainly affected by traction, braking force, and resistance during operation, as shown in

$$F = F_t + F_b + F_r, \tag{4}$$

where F is the resultant force of the train, F_t is the train traction force, F_b is the train braking force, and F_r is the train resistance; when the train is in traction condition, the value of F_b is zero and negative, the values of F_t and F_b are zero, F_r is negative in the coasting condition, the value of F_t is zero, and at the same time, F_r and F_b are negative in braking conditions.

Train resistance refers to the force opposite to the running direction of the train due to the influence of friction, impact, vibration, the plane and section of the line, and other external conditions during train operation. According to the causes, train resistance is divided into basic resistance, additional resistance, and starting resistance [26]. The following train operation processes under traction, coasting, and braking conditions are shown in

$$\begin{cases} F = F_t - F_r \\ a_t = \dfrac{F_t}{m} - \dfrac{g\left(c \cdot v_t^2 + b \cdot v_t + a\right)}{1000} \\ v_t = v_0 + \displaystyle\int_{t_0}^{t} a_t dt \\ s_t = \displaystyle\int_{t_0}^{t} v_t dt \end{cases}, \tag{5}$$

$$\begin{cases} F = -F_r \\ a_c = -\dfrac{g\left(c \cdot v_c^2 + b \cdot v_c + a\right)}{1000} \\ v_c = v_h + \displaystyle\int_{t_c}^{t} a_c dt \\ s_c = \displaystyle\int_{t_c}^{t} v_c dt \end{cases}, \tag{6}$$

$$\begin{cases} F = -F_r \\ a_c = -\dfrac{g\left(c \cdot v_c^2 + b \cdot v_c + a\right)}{1000} \\ v_c = v_h + \displaystyle\int_{t_c}^{t} a_c dt \\ s_c = \displaystyle\int_{t_c}^{t} v_c dt \end{cases}, \tag{7}$$

where a_t, v_t, and s_t are the acceleration, speed, and driving distance of the train in the traction condition, respectively, and v_0 and t_0 are the initial speed and time when the train starts. a_c, v_c, and s_c are the acceleration, speed, and driving distance of the train during coasting, v_h and t_c are the initial speed and time of the train during coasting, a_b, v_b, and s_b are

the acceleration, speed, and driving distance of the train under braking condition, and v_l and t_b are the initial speed and time of the train during braking.

3.2. Model Solving. According to the assumptions in the previous section of this paper, the leader train adopts the maximum traction force for traction, the maximum braking force for braking, and the coasting condition in the middle. The follower train adopts the maximum traction force for traction under the traction condition, enters the first coasting condition when reaching the set speed, and according to the coordination condition or coasting to the last moment that can meet the running time and running distance, retraction (traction equivalent to the braking force)-coasting braking (maximum braking force, parameter setting and solution steps are shown in Figure 2.

In Figure 2, v_{t2} and t_{t2}, respectively, represent the initial speed and time of secondary traction of urban rail trains; z_{stan} and n represent the total number of stations completed of urban rail trains and the total number of target operation stations, respectively. According to the operation steps of the leader train and the follower train, the premise of solving the train objective function is the operation sequence, that is, the solving equations. Once the operation sequence is changed, the train operation objective function needs to be recalculated and adjusted.

4. Consistency Agreement and Analysis

4.1. Consistency Agreement

Definition 1. If the state of the agent finally meets $\lim_{x \longrightarrow \infty} \|x_i(t) - x_0(t)\| = 0$ under any initial conditions, it is said that the system obtains master-slave consistency. The purpose of energy savings is achieved by the immediate utilization of braking regenerative energy. The total energy consumption of train i in a certain station is E_i, which is shown as follows:

$$E_i = E_t^i - E_b^{i0}, \tag{8}$$

$$E_t^i = \int_{t\in T} p_t^i(t)dt = \int_{t\in T} F_t^i(v_i,t)\cdot v_i(t)dt, \tag{9}$$

$$E_b^{i0} = \begin{cases} E_b^0 p_t^i(t) > p_b^0(t) \\ E_t^i p_t^i(t) = p_b^0(t) \\ E_t^i - E_b^0 p_t^i(t) < p_b^0(t) \end{cases}, \tag{10}$$

$$E_b^0 = \int_{t\in T} p_b^0(t)dt = \int_{t\in T} F_b^0(v_0,t)\cdot v_0(t)dt, \tag{11}$$

where E_t^i is the total traction energy consumption of the train, E_b^0 is the braking regenerative energy of the leader train, E_b^{i0} is the braking regenerative energy of the leader train absorbed by the train, $p_t^i(t)$ is the traction instantaneous power of trains, $p_b^0(t)$ is the braking instantaneous power of the leader train, $F_t^i(v_i,t)$ is the traction force of the train at the moment, and $F_b^0(v_0,t)$ is the braking force of the leader train at the moment; they can be expressed as follows:

$$F_t^i(v_i,t) = m_i\cdot a_i(t) + F_r^i(v_i,t), \tag{12}$$

$$F_b^0(v_0,t) = m_0\cdot a_0(t) - F_r^0(v_0,t), \tag{13}$$

where m_i is the mass of trains, $a_i(t)$ is the acceleration of trains, m_0 is the mass of the leader train, $a_0(t)$ is the acceleration of the leader train (negative value under braking condition), and $F_r^i(v_i,t)$ and $F_r^0(v_0,t)$ are the basic running resistances of the follower train and the leader train, respectively; they can be expressed as follows:

$$F_r^i(v_i,t) = m_i\cdot F_{ur}^i(v_i,t)g\cdot 10^{-3}\,(i=0,1,2\cdots), \tag{14}$$

$$F_{ur}^i(v_i,t) = a + b\cdot v_i(t) + cv_i^2(t). \tag{15}$$

Here, $F_{ur}^i(v_i,t)$ is the unit of the basic running resistance of the train, g is the gravitational acceleration, and a, b, and c are the empirical parameters determined by the experiment, respectively. Multitrain energy-saving cooperative following consistency can be described as follows:

$$\lim_{t\longrightarrow\infty}\left\|\mu a_i(t) - \lambda a_0(t))\right\| = 0, \tag{16}$$

where a_0 is the acceleration of the leader train, a_i is the acceleration of train i, and μ and λ are both energy-saving synergy coefficients; generally, μ is any real number, $\lambda = 1$. β_i is defined as the difference between the weighted acceleration value of the following train i and the weighted acceleration value of the leader train. β_i is called the collaborative deviation degree, which is recorded as $\beta_i = \mu a_i - \lambda a_0$. During the actual operation of the train, we do not need the acceleration of each train to be completely consistent with the acceleration of the leader. When the acceleration state meets our requirements, we can also consider that a collaborative agreement is reached, that is, $\beta_i \le \varepsilon$; the multitrain system reaches coordination, where ε is the synergetic error.

Based on the consistent design objective, the system regulation coefficient γ is introduced and the event driving function is defined, as shown in the following equation:

$$\left\|e_i(t)\right\| \le \gamma\left\|q_i\left(t_k^i\right)\right\|. \tag{17}$$

If equation (17) does not hold, the system will update the controller; otherwise, the system will not be driven. $e_i(t) = q_i(t_k^i) - q_i(t)$ is the error function of the system at time t. The system regulation parameter γ shall meet $0 < \gamma < 1$.

A control protocol with input saturation can be designed by the driving function, as shown in the following equation:

$$u_i(t) = -Kq_i\left(t_k^i\right) = -\alpha K\left(x_i\left(t_k^i\right) - x_0\left(t_{\overline{k}}^{\,0}\right)\right). \tag{18}$$

Since the negotiation variable is train acceleration, (18) can be converted into the following equation:

$$u_i(t) = -Kq_i\left(t_k^i\right) = -\alpha K\left(\mu a_i\left(t_k^i\right) - \lambda a_0\left(t_{\overline{k}}^{\,j}\right)\right), \tag{19}$$

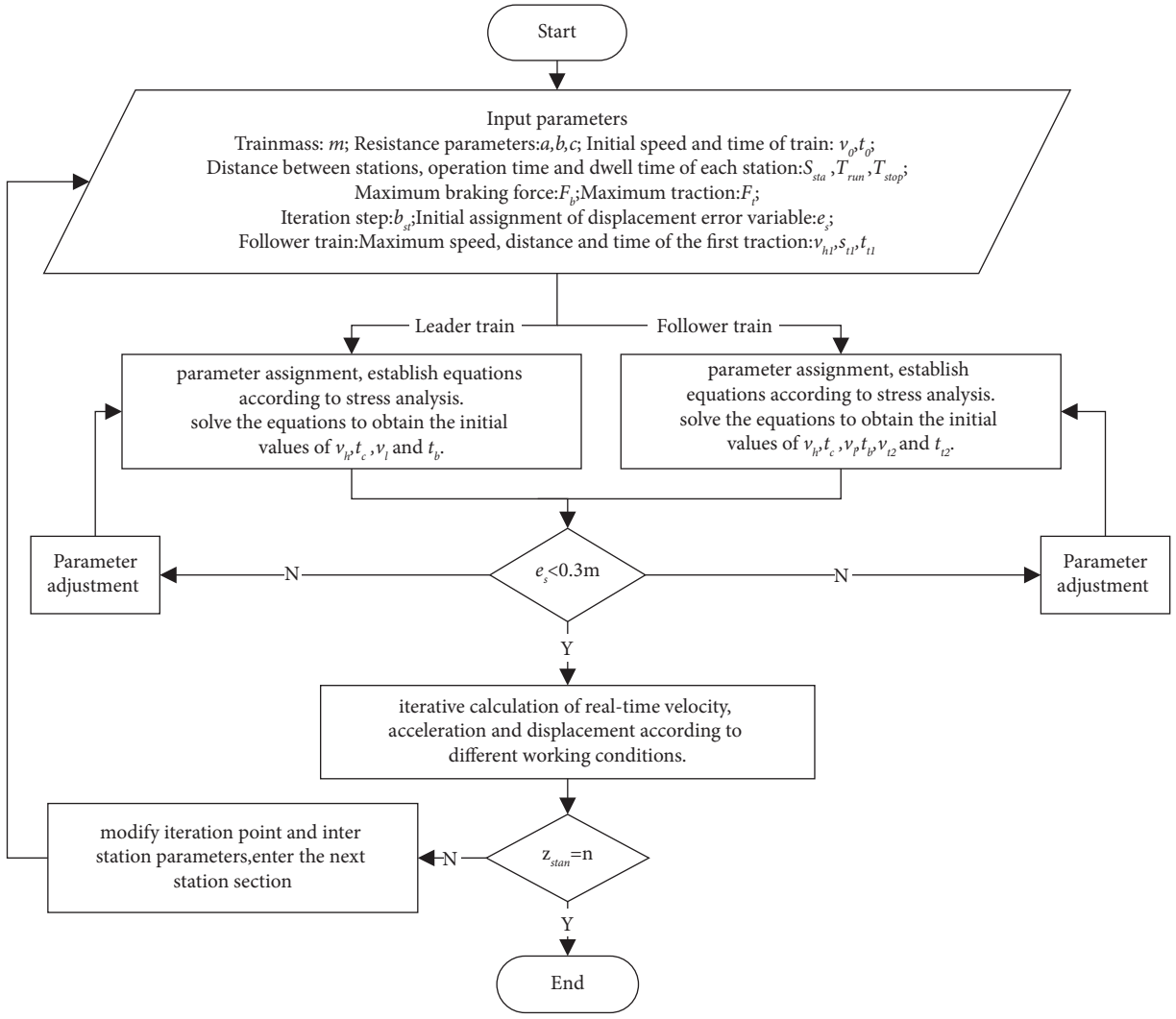

Figure 2: Parameter setting and solution steps.

where $t \in [t_k^i, t_{k+1}^i)$, t_k^i and $t_{\bar{k}}^0$ are the event-driven event sequences of the train and the leader train, respectively, k and $\bar{k}$ are positive integers, K is the control gain matrix, and α represents constants greater than 0.

Since the leader train is not affected by the consistency protocol, only the follower train is considered in the research process and the control structure of the follower train i is shown in Figure 3.

4.2. Consistency Analysis

Lemma 1 (see [27]). *It is supposed that for a set* $R_\zeta = \{v, z: \|v - v_z\| \le u_{oi}, \forall i = 1, 2, \cdots, n\}$, *where* $v \in R^p$ *and* $z \in R^p$ *are vector elements in* R_ζ, *there is a dead zone nonlinear function* $\phi(v)$, *so that the* $\phi(v)^T T(\phi(v) + z) \le 0$ *inequality holds, where* $\in R^{p\times p}$ *is any positive definite diagonal matrix. The condition provides a feasible basis for transforming the system stability problem into an LMI solution problem.*

Theorem 1. *Considering equations (1) and (2), it is supposed that the topological graph of the system is a strongly connected graph and contains a directed spanning tree, if there is a positive definite matrix* $P \in R^{n\times n}$, *any diagonal positive definite matrix* $T \in R^{p\times p}$, *matrix* $G \in R^{m\times m}$, *matrix* $\in R^{m\times m}$, *a positive number* η, *and two positive scalars* τ_1 *and* τ_2, $0 < \gamma < 1$; *these satisfy the following equations:*

$$\begin{bmatrix} I_n \otimes PG_i^T \\ * \quad \eta u_{oi}^2 \end{bmatrix} \ge 0, \tag{20}$$

$$\begin{bmatrix} a_{11} I_N \otimes PB + TKH - TGI_N \otimes PBK \\ * \quad -2(I_m \otimes T)TK \\ * \quad -\tau_2 I_{Nm} \end{bmatrix} < 0, \tag{21}$$

where $a_{11} = (I_N \otimes PA) + (I_N \otimes A^T P) - 2(H \otimes PBK) + \tau_1 (IP) + \sigma(I_m \otimes H^T)(I_m \otimes H)$, $H = L + B$, *and* $\sigma = \tau_2 (\gamma/1 - \gamma)^2$. *Then, the error trajectory of the follower and the leader will be included in this ellipsoid; that is, the follower can achieve the desired consistency.*

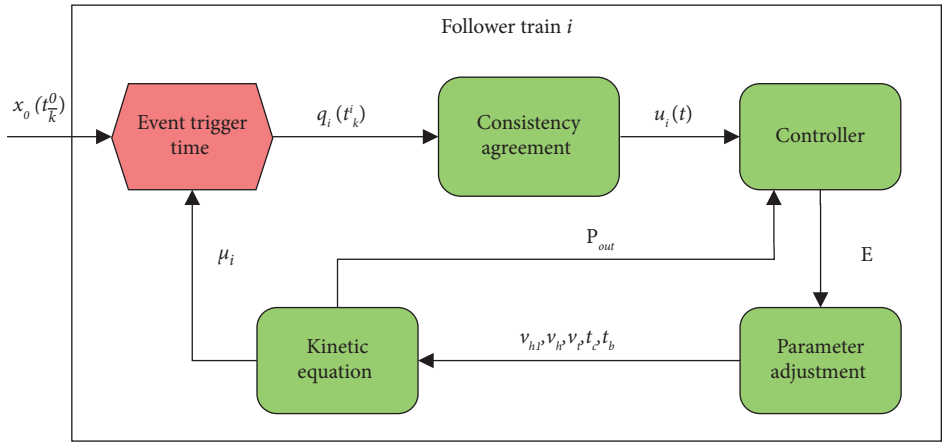

Figure 3: Control structure diagram of the follower train.

Prove: in vector $\hat{\hat{x}}(t) = (\hat{\hat{x}}_1(t), \hat{\hat{x}}_2(t), \cdots \hat{\hat{x}}_N(t))$, $\hat{\hat{x}}_i(t) = x_0(t) - x_i(t)$ *represents the state error* $e(t) = (e_1(t), e_2(t), \cdots e_N(t))^T$ *root of the ith follower and leader; then, the error system can be shown in the following equation:*

$$\dot{\hat{\hat{x}}}(t) = (I_N \otimes A)\hat{\hat{x}}(t) + Bsat(-KH\hat{\hat{x}}(t) - Ke(t)), \tag{22}$$

where $H = L + B$ *and the dead zone nonlinear function* $\phi(\cdot)$ *will be introduced to replace the saturated nonlinear function; if* $\phi(u(t)) = sat(u(t)) - u(t)$, *then (22) can be converted into the following equation:*

$$\begin{aligned}\dot{\hat{\hat{x}}}(t) = {} & (I_N \otimes A)\hat{\hat{x}}(t) + (I_N \otimes B)\phi(-KH\hat{\hat{x}}(t) - Ke(t)) \\ & - (H \otimes BK)\hat{\hat{x}}(t) - (I_N \otimes BK)e(t).\end{aligned} \tag{23}$$

From event-driven function (17), the following can be obtained:

$$\|e_i(t)\| \le \gamma\|q_i(t) + e_i(t)\| \le \gamma\|q_i(t)\| + \gamma\|e_i(t)\|, \tag{24}$$

$$\|e_i(t)\| \le \frac{\gamma}{1-\gamma}\|q_i(t)\|. \tag{25}$$

Therefore, it can be obtained that (26) is valid.

$$e^T(t)e(t) \le \left(\frac{\gamma}{1-\gamma}\right)^2 \left[(I_m \otimes H)\hat{\hat{x}}\right]^T \left[(I_m \otimes H)\hat{\hat{x}}\right]. \tag{26}$$

Lyapunov function is selected for stability analysis;we assume that (27) holds.

$$V = \hat{\hat{x}}^T (I_N \otimes P)\hat{\hat{x}}, \tag{27}$$

where P is a positive definite symmetric matrix because it is stable, and the equation $A^TP + PA - PBB^TP + I_n = 0$ has a unique positive definite solution. To prove the stability of (22), it is necessary to prove that function (27) $\dot{V} \le 0$ is satisfied; that is, it is necessary to prove that for any $\hat{\hat{x}} \notin \text{int}, R_\zeta$ and e are established under equation (17), $\dot{V} \le 0$ satisfying the driving conditions.

The S-procedure method can transform the problems that do not belong to convex constraints into linear matrix inequality constraints, so it is convenient to solve them by using linear matrix inequality [28].

> Order: σ_k: $V \longrightarrow R(k = 0, 1, \cdots, N)$ is a real valued objective function defined on the linear vector space V, with the following two conditions. $S1$: for any $\in V$, $\sigma_0(y) \ge 0$ and the constraint condition is $\sigma_k(y) \ge 0$; $S2$: if $\tau_k \ge 0$, then $\sigma_0 - \sum_{k=1}^N \tau_k\sigma_k(y) \ge 0$ and $\forall y \in V$. Suppose
>
> $S1$: $\dot{V} \le 0$, s.t.$\hat{\hat{x}}^T(I_n \otimes P)\hat{\hat{x}} > \eta^{-1}$, $\|e_i(t)\| \le \gamma\|q_i(t_k^i)\|$
>
> $S2$: $\dot{V} + \tau_1(\hat{\hat{x}}^T P\hat{\hat{x}} - \eta^{-1}) + \tau_2((\gamma/1-\gamma)^2((I_m \otimes H)\hat{\hat{x}}^T ((I_m \otimes H)\hat{\hat{x}}) - e^Te) < 0$

According to the ss-procedure method, the premise of proving $S1$ is to prove $S2$. Therefore, $S2$ can be simplified to an equation.

$$\dot{V} + \tau_1\left(\hat{\hat{x}}^T P\hat{\hat{x}} - \eta^{-1}\right) + \sigma((I_m \otimes H)\hat{\hat{x}}^T (I_m \otimes H)\hat{\hat{x}} - \tau_2\left(e^Te\right) < 0, \tag{28}$$

where $\sigma = \tau_2(\gamma/1-\gamma)^2$; suppose $v = u$, $z = u + G\hat{\hat{x}}$; for any $\hat{\hat{x}} \in S = \left\{\hat{\hat{x}}: |G_i\hat{\hat{x}}| \le u_{oi}, \forall i = 1, 2, \cdots, n\right\}$ can satisfy the conditions in Lemma 1, that is $\phi'(u)T(\phi(u) + u + G\hat{\hat{x}}) \le 0$; the establishment of LMI can ensure the ellipsoid $R_\zeta \subset S$ [27]. To prove that $\dot{V} \le 0$ is true, only (29) needs to be proved to be true.

$$\dot{V} + \tau_1\hat{\hat{x}}^T (I_N \otimes P)\hat{\hat{x}} + \sigma(H\hat{\hat{x}})^T (H\hat{\hat{x}}) - \tau_2e^Te - 2\phi^T(u)T(\phi(u) + u + G\hat{\hat{x}}) < 0. \tag{29}$$

Namely,

$$\begin{aligned}&2\hat{x}^T(I_N\otimes PA)\hat{x}+2\hat{x}^T(I_N\otimes PB)\phi(u)-2\hat{x}^T(H\otimes PB)K\hat{x}-2\hat{x}^T(I_N\otimes P(BK))e\\&+\tau_1\hat{x}^T(I_N\otimes P)\hat{x}+\sigma\hat{x}^TH^TH\hat{x}-\tau_2e^Te-2\phi^T(u)T\phi(u)+2\phi^T(T\otimes KH)\hat{x}\\&+2\phi^T(u)TKe-2\phi^T(u)TG\hat{x}<0.\end{aligned}\tag{30}$$

Suppose $\varepsilon(t)=(\hat{x}^T(t)\phi^T(u)e^T(t))$; we just prove that $\varepsilon^T\prod_1\varepsilon<0$. Among them,

$$\prod_1=\begin{bmatrix}a_{11} & I_N\otimes PB+TKH-TG & I_N\otimes P(BK)\\ * & -2(I_m\otimes T) & TK\\ * & * & -\tau_2I_{N\times m}\end{bmatrix},\tag{31}$$

where $a_{11}=(I_N\otimes PA)+(I_N\otimes A^TP)-2(H\otimes P(PK))+\tau_1(I_N\otimes P)+\sigma(I_m\otimes H^T)(I_m\otimes H)$; therefore, according to Lyapunov's asymptotic stability theorem, the error system is asymptotically stable; that is, the follower and the leader achieve the desired consistency.

To show that there is no Zeno phenomenon in the whole event-triggering control process, reference [16] gives the following definitions.

Definition 2. If the event driving interval meets the conditions $\inf_k\{t_{k+1}^i-t_k^i\}>0$, the system can eliminate the Zeno phenomenon;that is, the system will not be infinitely triggered within the limited driving time.

Theorem 2. *Consider master-slave systems (1) and (2), in which communication topology is strongly connected. Based on the event-driven control protocol (19) and driving condition (17), each train can obtain the initial state of other trains at the initial time and each train can transmit the driving time state information to other trains; then, all trains applying control protocol (19) and driving conditions (17) will not generate the Zeno phenomenon.*

Prove: because $\|e_i(t)\|\le\gamma/1-\gamma\|q_i(t)\|$, we can get $\|e_i(t)\|\le\gamma/1-\gamma\|H\hat{x}\|$; from $\dot{e}_i(t)=-\dot{q}_i(t)=-(H\otimes A)\overline{x}(t)-(H\otimes B)u(t)$, we will get

$$|e_i(t)|\le\int_f^{t_k^it}\left|(H\otimes A)\hat{x}_i(s)(H\otimes B)u_i(s)\right|ds.\tag{32}$$

Since there is (33) and $\|\hat{x}(t)\|_\infty=\sup_{t\ge0}\|\hat{x}(t)\|$, (32) can be changed into

$$\begin{aligned}&\left|(H\otimes A)\hat{x}_i(t)+(H\otimes B)u_i(t)\right|\le\|(H\otimes A)\hat{x}(t)+(H\otimes B)u(t)\|\\&\le\|H\otimes A\|\|\hat{x}(t)\|+\|H\otimes B\|\|u(t)\|\le\|H\otimes A\|\|\hat{x}(t)\|+\|H\otimes B\|\|HK\|\left\|\hat{x}\left(t_k^i\right)\right\|\end{aligned}\tag{33}$$

$$|e_i(t)|\le\left(t-t_k^i\right)\times\left(\|H\otimes A\|\|\hat{x}(t)\|_\infty+\|H\otimes B\|\|HK\|\left\|\hat{x}\left(t_k^i\right)\right\|\right).\tag{34}$$

Formula (35) is valid.

$$\left(t-t_k^i\right)\ge\frac{|e_i(t)|}{\|H\otimes A\|\|\hat{x}(t)\|_\infty+\|H\otimes B\|\|HK\|\left\|\hat{x}\left(t_k^i\right)\right\|}.\tag{35}$$

When the system is driven, (36) can be established.

$$|e(t)|>\frac{\gamma}{1-\gamma}\|H\hat{x}\|.\tag{36}$$

Because $0<\gamma<1$ exists, the system will have $|e(t)|>0$ when driven, that is,

$$\left(t_{k+1}^i-t_k^i\right)\ge\frac{|e_i(t)|}{\|H\otimes A\|\|\hat{x}(t)\|_\infty+\|H\otimes B\|\|HK\|\left\|\hat{x}\left(t_k^i\right)\right\|}>0.\tag{37}$$

To sum up, if the event driving interval is greater than zero, the system can eliminate the Zeno phenomenon and Theorem 2 is proved.

5. Simulation and Analysis

A MATLAB simulation is used to verify the correctness of the theoretical scheme. The number of trains in the system is set to 4, including 1 leader and 3 followers. The train

Table 1: Running distance between stations.

Station	Station 1	Station 2	Station 3	Station 4	Station 5	Station 6	Station 7	Station 8	Station 9	Station 10	Station 11	Station 12
Distance (m)	1850	2030	1558	1302	1395	1845	1753	2330	2105	2880	1560	2338

Table 2: The train operation parameters.

Train weight (t)	Maximum speed (km/h)	Maximum traction (kN)	Maximum braking (kN)	Maximum traction acceleration (m/s^2)	Maximum braking acceleration (m/s^2)	Basic resistance parameters
194	80	195	160	1	0.9	$a = 2.031$ $b = 0.0622$ $c = 0.001807$

Table 3: Value of coordination coefficient.

Leader train working condition	Value of follower train coordination coefficient
Traction condition	$\mu_i = \begin{cases} 1 & \text{when train } i \text{ is under traction condition} \\ -24 & \text{when train } i \text{ is under coasting condition} \\ -1 & \text{when train } i \text{ is under braking condition} \end{cases}$
Coasting condition	$\mu_i = \begin{cases} -0.04 & \text{when train } i \text{ is under traction condition} \\ 1 & \text{when train } i \text{ is under coasting condition} \\ 0.04 & \text{when train } i \text{ is under braking condition} \end{cases}$
Braking condition	$\mu_i = \begin{cases} -1 \text{ when train } i \text{ is under traction condition} \\ -1 \text{ when train } i \text{ is under 1th coasting condition} \\ 24 \text{ when train } i \text{ is under 2th coasting condition} \\ 1 \quad \text{when train } i \text{ is under braking condition} \end{cases}$

operation diagram refers to a part of a certain line of a subway operation company. The distance between stations of train operations is shown in Table 1, and the train operation parameters are shown in Table 2.

It can be seen from Tables 1 and 2 that, under the premise of not changing the system operation time, the research does not need to consider train safety. Set train 0 as the leader train (the leading train) and train 1, train 2, and train 3 as the following train (the following train). The leader train 0 operates in the optimal operation sequence of a single train, and the follower trains 1, 2, and 3 operate in the cooperative energy-saving optimal operation sequence. The set parking accuracy is not greater than 0.3 m, and the punctuality is less than 1 s. The acceleration is regarded as a collaborative variable, and a consistency protocol is introduced, along with its energy-saving synergy coefficient $\lambda = 1$ and $\varepsilon = 0.2$. The value of u_i is shown in Table 3.

It can be seen from Table 3 that only under first inert working condition can the follower train carry out the following consistency coordinated control.

Then, the operation curve of 4 trains can be obtained, as shown in Figure 4.

As can be seen from Figure 4, the following train 1 runs between station 8 and station 9, train 2 runs between station 1 and station 2, between station 2 and station 3, between station 6 and station 7, and between station 8 and station 9, and train 3 runs between station 1 and station 2, between station 2 and station 3, and between station 6 and station 7. The follower train is affected by the acceleration change of the leader train between the corresponding station areas, and its weighted acceleration follows consistently. With the change of its working condition transition point, the secondary traction is carried out at the event trigger time (the leader train braking time), and the follower train starts to absorb and utilize the regenerative braking energy of the leader train. Energy-saving optimization is carried out on the premise of ensuring operation time and train parking accuracy. The variation trend of consistency coordination deviation β_i is shown in Figure 5.

As shown in Figure 5, the follower train realizes ε coordination and the trigger time of the follower train is shown in Figure 6, which greatly reduces the system communication frequency and avoids the waste of network resources.

According to equations (8)–(11), the energy consumed and regenerative energy of the follower train before and after consistency control to complete the above simulation events are given, as shown in Table 4.

Figure 7 shows the energy consumption of the follower train.

It can be seen from Figure 7(a) that the newly added follower train 1 absorbs and utilizes the regenerative energy of the leader train when it operates between stations 8 and 9. It can be seen from Figure 7(b) that the newly added follower train 2 absorbs and utilizes the regenerative energy of the leader train when it operates between stations 1 to 2 and 2 to 3. The newly added follower train absorbs and utilizes the regenerative energy of the leader train when it operates between stations 6 to 7 and 8 to 9, as shown in Figure 7(c). It

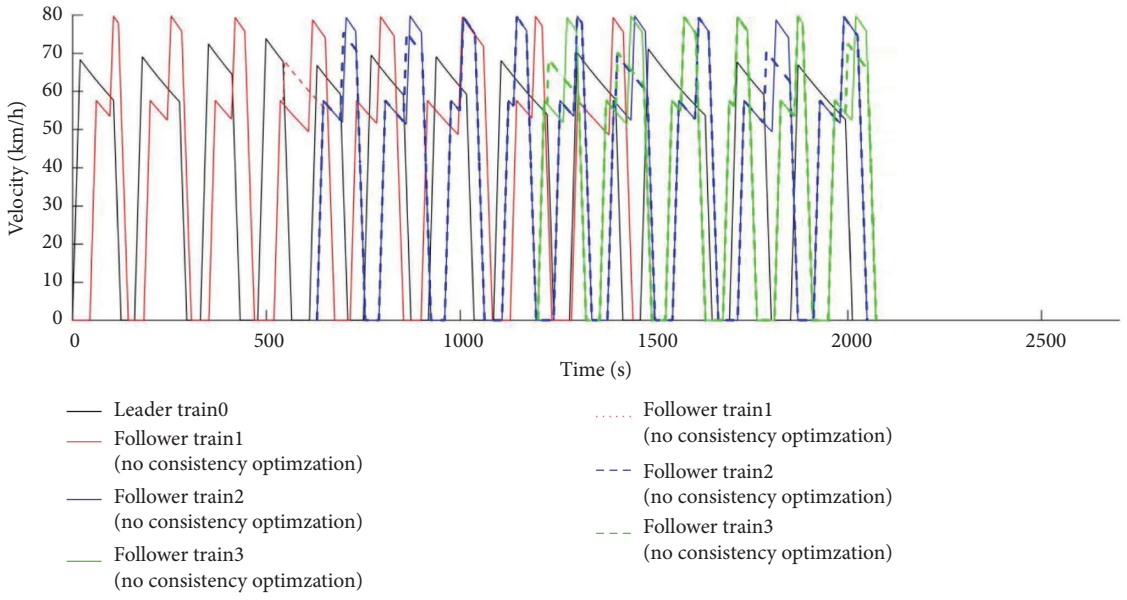

(a)

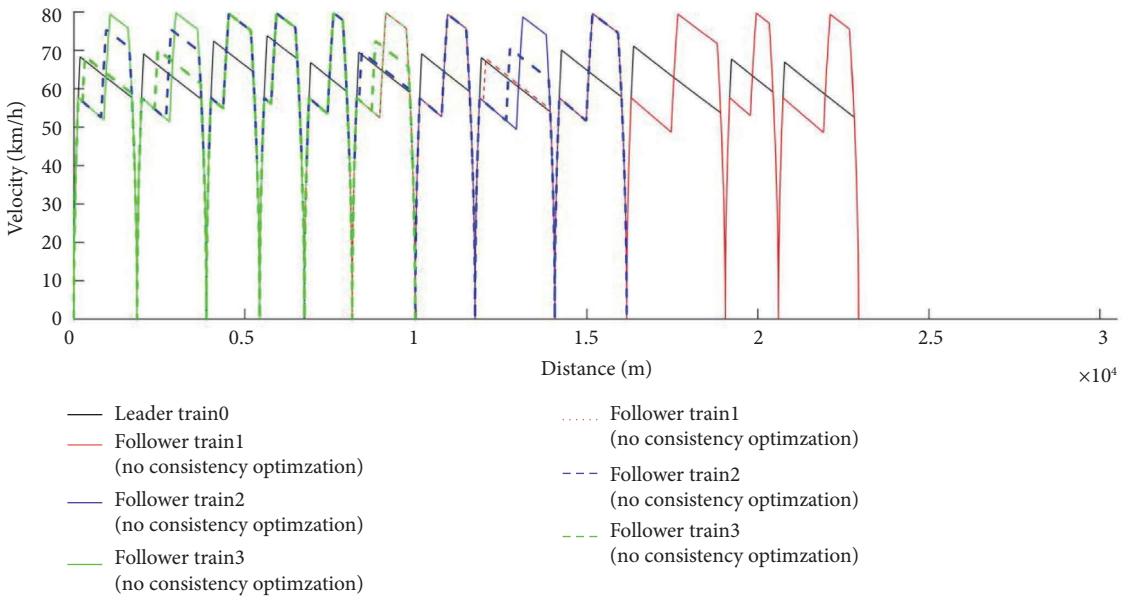

(b)

Figure 4: Continued.

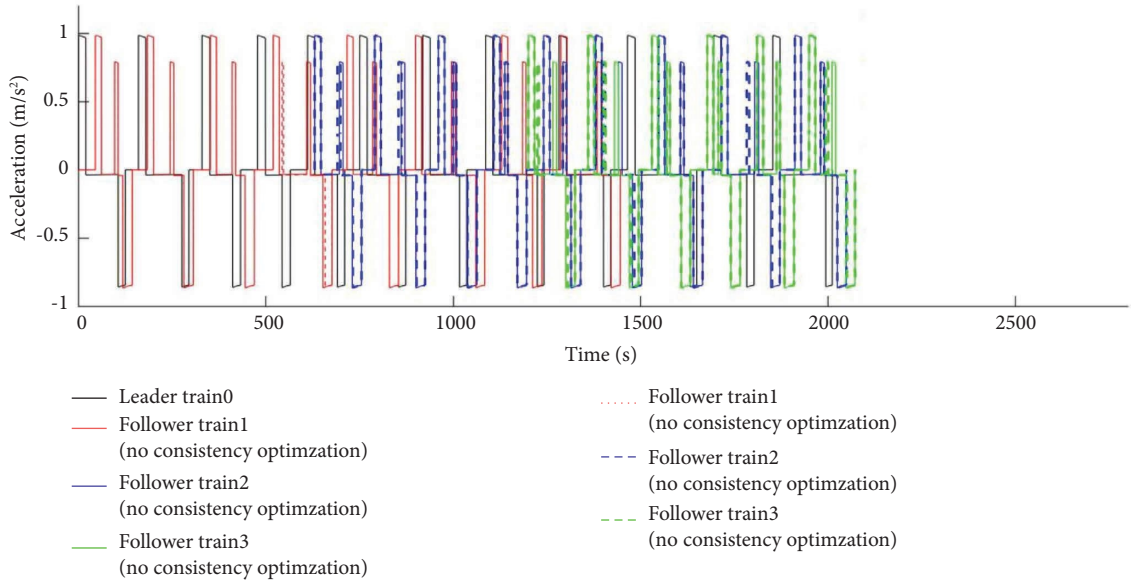

(c)

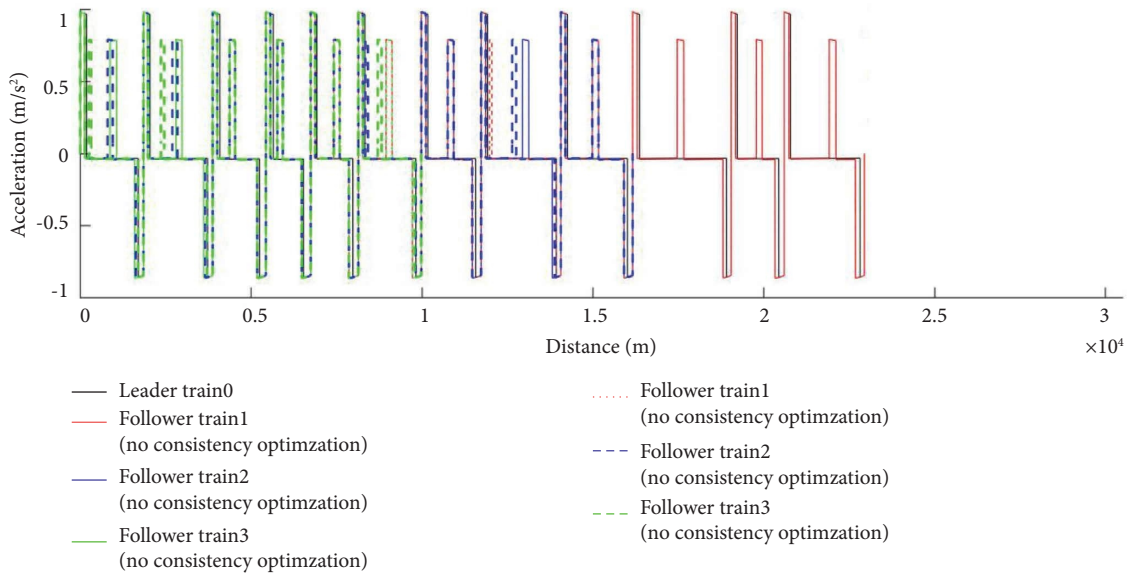

(d)

Figure 4: Continued.

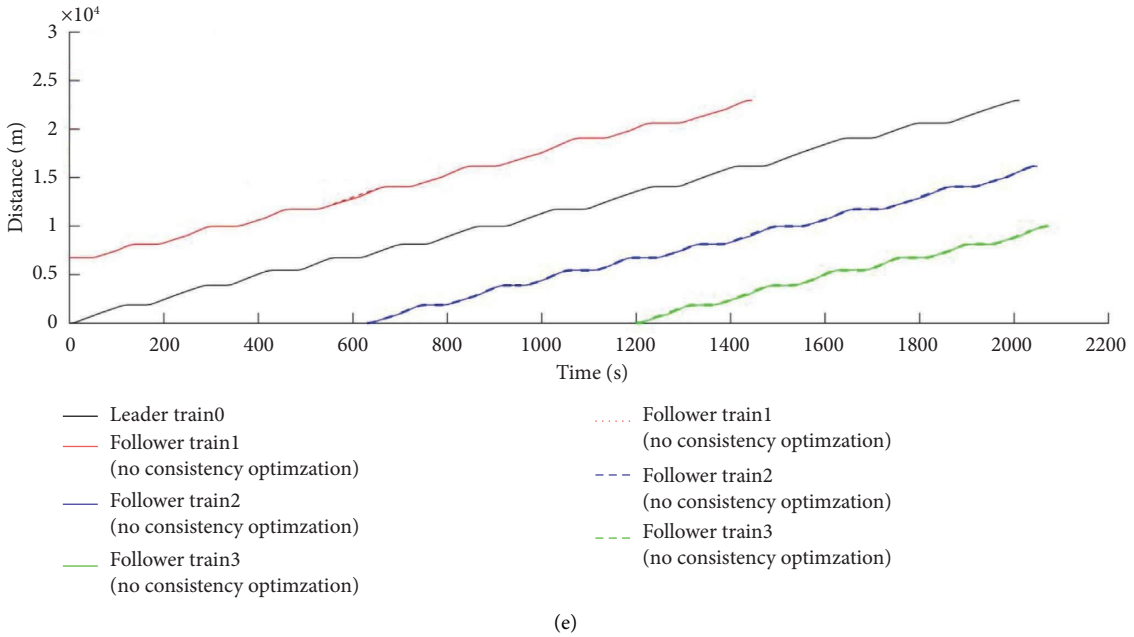

(e)

Figure 4: Running curves of 4 trains under consistent coordination state. (a) Time-velocity curve, (b) distance-velocity curve, (c) time-acceleration curve, (d) distance acceleration, and (e) time-distance curve.

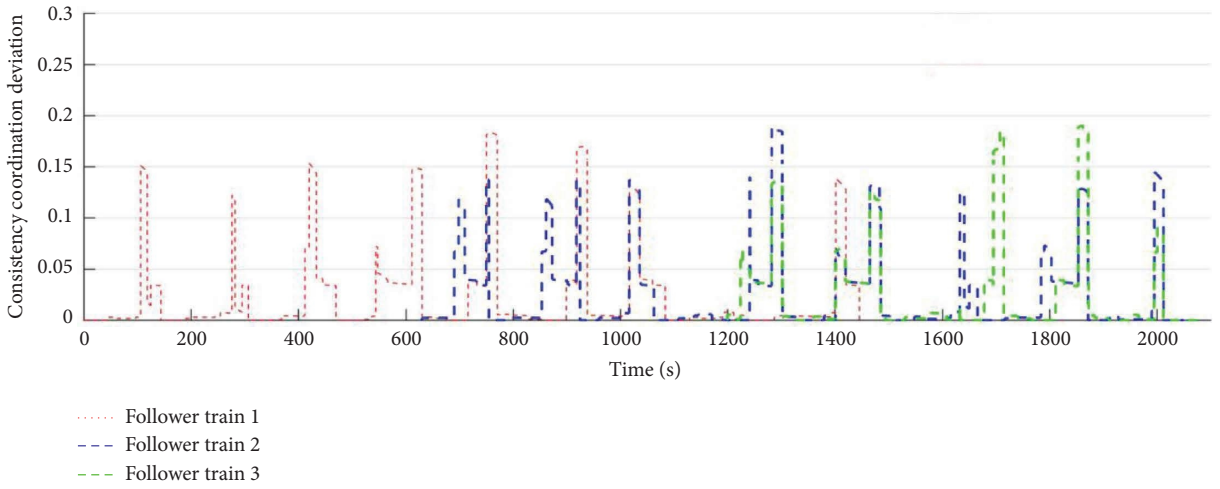

Figure 5: Variation trend of consistency coordination deviation β_i.

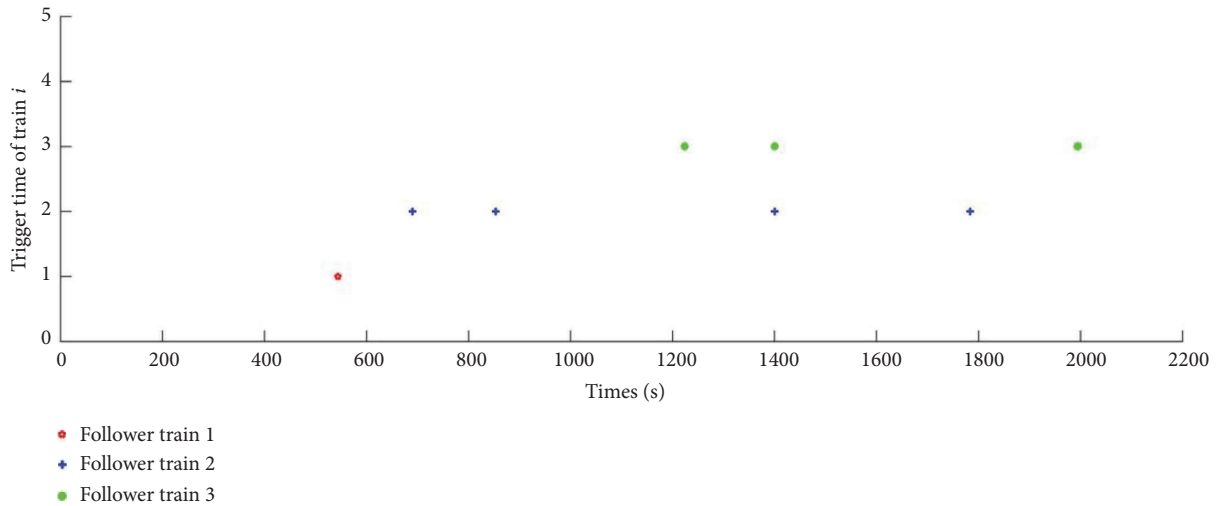

Figure 6: Train trigger time.

Table 4: Energy consumption of train operation.

Index	Before consistency control	After consistency control
Traction energy consumption of train 1/(kw·h)	121.80	116.60
Regenerative energy utilized by train 1/(kw·h)	4.92	7.45
Actual energy consumption of train 1/(kw·h)	116.88	109.15
Traction energy consumption of train 2/(kw·h)	134.25	123.40
Regenerative energy utilized by train 2/(kw·h)	6.11	15.33
Actual energy consumption of train 2/(kw·h)	128.14	108.07
Traction energy consumption of train 3/(kw·h)	88.81	77.23
Regenerative energy utilized by train 3/(kw·h)	0.06	8.04
Actual energy consumption of train 3/(kw·h)	88.75	69.19
Total traction energy consumption/(kw·h)	344.86	317.23
Total regeneration energy consumption/(kw·h)	11.09	30.82
Total actual energy consumption/(kw·h)	333.77	286.41

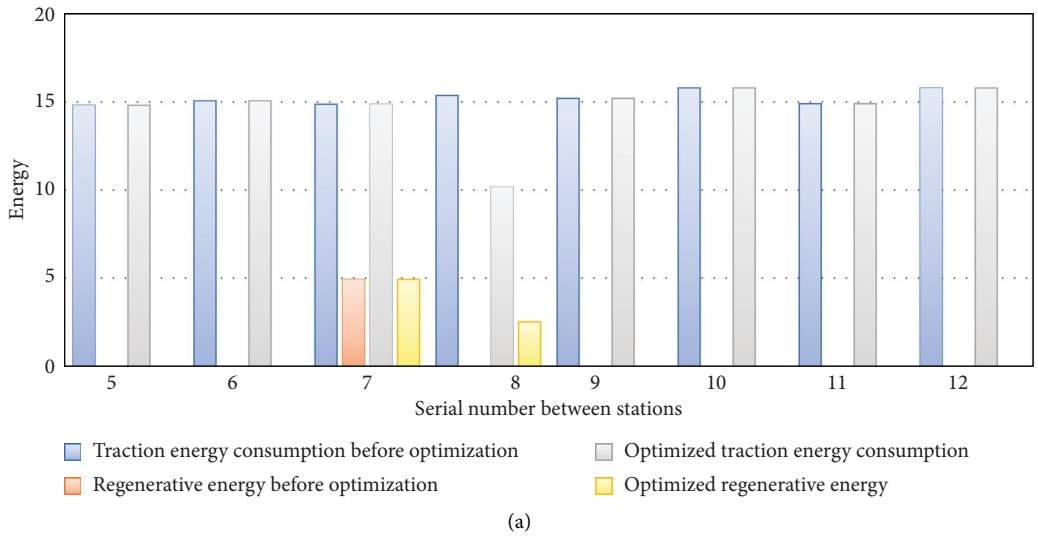

(a)

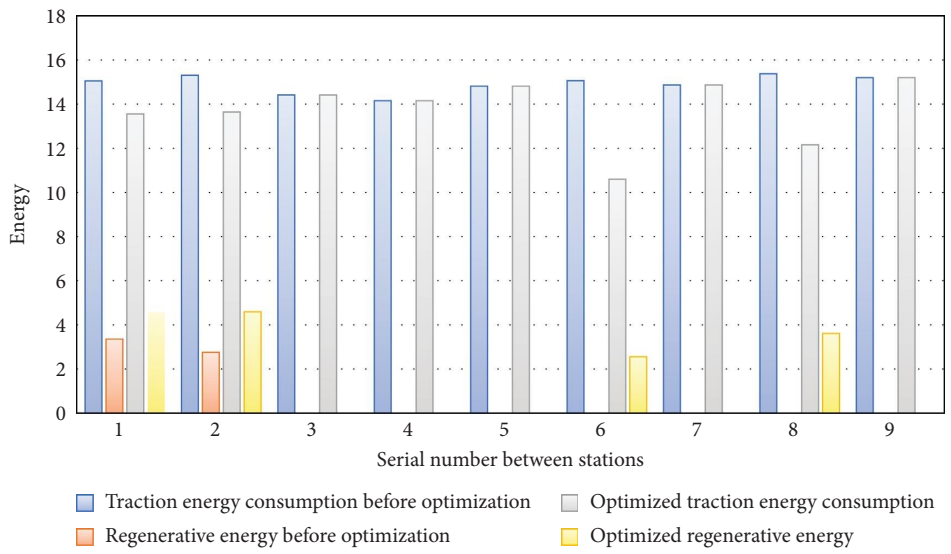

(b)

Figure 7: Continued.

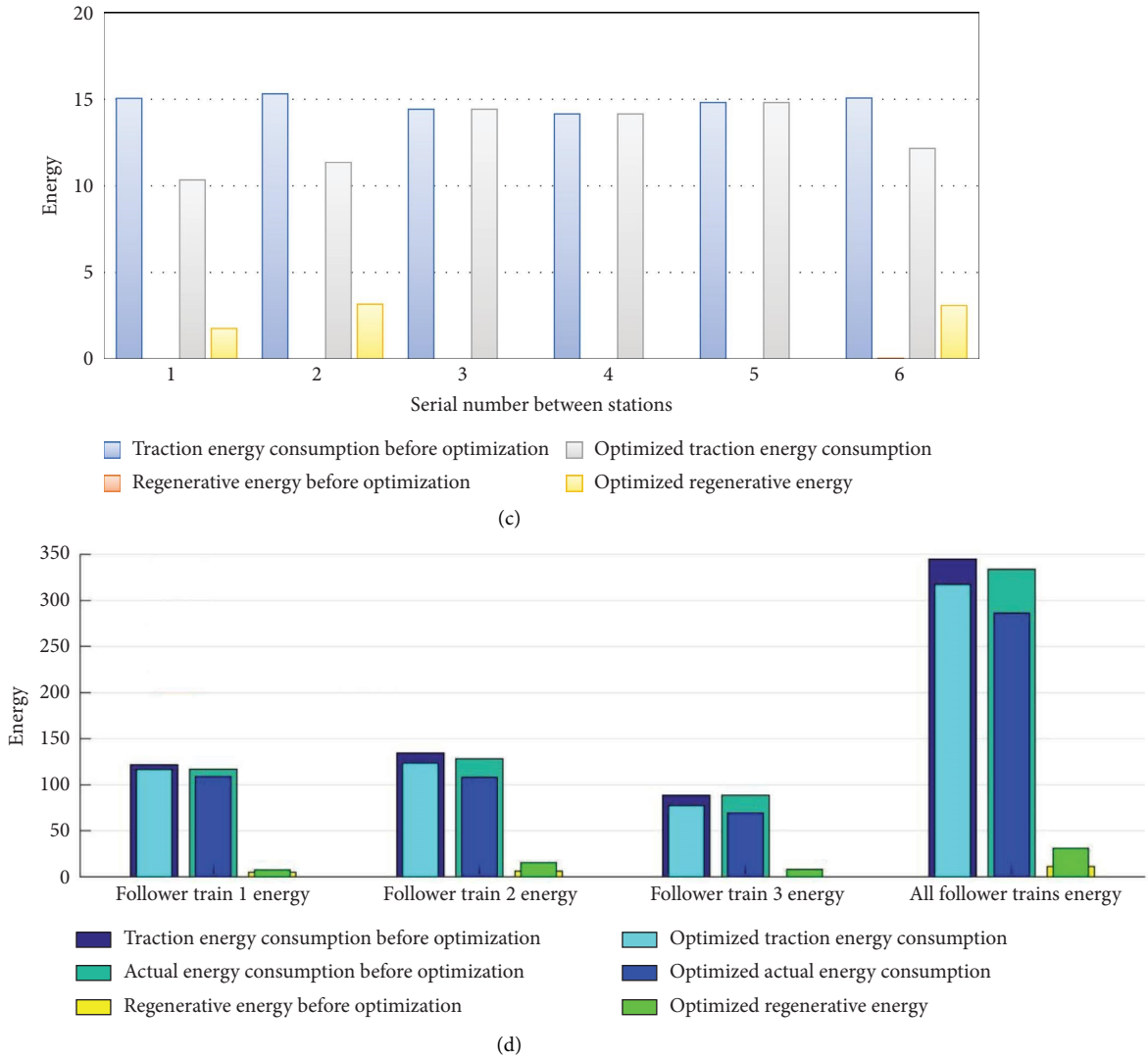

Figure 7: Energy consumption and regenerative energy utilization of follower trains: (a) energy consumption and regenerative energy utilization of train 1 between stations, (b) energy consumption and regenerative energy utilization of train 2 between stations, (c) energy consumption and regenerative energy utilization of train 2 between stations, and (d) total energy consumption and regenerative energy utilization of the following train during the running time.

can be seen that when follower train 3 operates between stations 6 and 7, its absorbed regenerative energy has been improved in detail, and the newly added regenerative energy is absorbed and utilized by the leader train when it operates between stations 1-2 and 2-3. This is consistent with the operation interval of the follower train and the leader train in Figure 4. It can be seen from Table 4 and Figure 7(d) that, on the premise of ensuring the parking accuracy and punctuality of the original train diagram, after the consistency optimization, the regenerative energy absorbed and utilized by each follower train has been improved to varying degrees and the proportion of the total utilized regenerative energy in the actual energy consumption has increased from 3.32% before optimization to 10.76% after optimization.

6. Conclusions

Taking the urban rail train as the research object, this paper establishes the energy-saving operation model of the urban rail train and studies the following consistency of urban rail train cooperative control. It is assuming that each urban rail vehicle is an agent, the synergy coefficient and synergy deviation degree are introduced, and the train acceleration is taken as the negotiation variable to study the feasibility of the follower train to achieve synergy. To save network resources and the amount of calculations of train coordination consistency, when designing the follower train consistency protocol, make each follower vehicle update the cooperative controller only at the time of event triggering. Through the

consistency analysis, it is proved that the multitrain system can achieve the leader following consistency under the consistency protocol, and the Zeno phenomenon is eliminated. Finally, it is verified by referring to the train diagram of a certain line of a subway operation company. Through simulation analysis, based on the energy-saving method proposed in this paper, on the premise of ensuring the original parking accuracy and punctuality, the proportion of the total renewable energy used by the follower train in the actual energy consumption is increased from 3.32% to 10.76%, reducing 9.23% of the actual total energy consumption of the train. The proposed method improves the utilization rate of regenerative energy of the leader train. Considering the leader following consistency under switching topology is the next key research content, which can expand the utilization range of renewable energy and further save traction energy consumption.

Data Availability

The data used to support the findings of this study were supplied under license and so cannot be made freely available. Requests for access to these data should be made to the corresponding author.

Conflicts of Interest

The authors declare that there are no conflicts of interest regarding the publication of this paper.

Acknowledgments

This work was supported by the National Natural Science Foundation of China (NSFC) under Grants 72061021 and 62063013, Science and Technology Plan Project of Gansu (20JR10RA251 and 21JR7RA284), Youth Fund Project of Lanzhou Jiaotong University (2021018).

References

[1] S. Li, J. Miao, L. Meng, J. Cong, and Y. Zhang, "Optimization of urban rail transit segment running time based on energy saving," *Journal of Railway Science and Engineering*, vol. 13, no. 8, pp. 1630–1635, 2016.

[2] P. Liu, *Research on Energy-Efficient Train Timetable Optimization Based on Regenerative Braking Energy in Urban Rail Transit*, Beijing Jiaotong University, China, 2020.

[3] Y. Bai, B. Yuan, J. Li, Y. Zhou, and X. Feng, "Cooperative control strategy for energy saving operation of metro train based on rolling optimization," *China Railway Science*, vol. 41, no. 3, pp. 163–170, 2020.

[4] A. Nasri, M. F. Moghadam, and H. Mokhtari, "Timetable optimization for maximum usage of regenerative energy of braking in electrical railway systems," in *Proceedings of the International Symposium on Power Electronics Electrical Drives Automation and Motion*, pp. 1218–1221, Pisa, Italy, 14-16 June 2010.

[5] M. P. Alcaraz, A Fernandez, A. P. Cucala, A. Ramos, and R. R. Pecharroman, "Optimal underground timetable design based on power flow for maximizing the use of regenerative braking energy," *Proceedings of the Institution of Mechanical Engineers - Part F: Journal of Rail and Rapid Transit*, vol. 226, no. 4, pp. 397–408, 2012.

[6] S. Su, X. Li, T. Tang, and Z. Gao, "A subway train timetable optimization approach based on energy efficient operation strategy," *IEEE Transactions on Intelligent Transportation Systems*, vol. 14, no. 2, pp. 883–893, 2013.

[7] J. Liu, H. Guo, and Y. Yu, "Research on the cooperative train control strategy to reduce energy consumption," *IEEE Transactions on Intelligent Transportation Systems*, vol. 18, no. 5, pp. 1134–1142, 2017.

[8] J. Xun, T. Tang, X. Song, B. Wang, and Z. Jia, "Comprehensive model for energy-saving train operation of urban mass transit under regenerative brake," *China Railway Science*, vol. 36, no. 1, pp. 104–110, 2015.

[9] X. Sun, H. Lu, and H. Dong, "Energy-efficient train control by multi-train dynamic cooperation," *IEEE Transactions on Intelligent Transportation Systems*, vol. 18, no. 11, pp. 3114–3121, 2017.

[10] Y. Cao, *Study on Energy Saving Method of Subway Train Cooperative Control*, Beijing Jiaotong University, China, 2017.

[11] Z. Zhang, F. Hao, L. Zhang, and L. Wang, "Consensus of linear multi-agent systems via event-triggered control," *International Journal of Control*, vol. 87, no. 6, pp. 1243–1251, 2014.

[12] Z. W. Liu, Z. H. Guan, X. Shen, and G. Feng, "Consensus of multiagent networks with aperiodic sampled communication via impulsive algorithms using position-only measurements," *IEEE Transactions on Automatic Control*, vol. 57, no. 10, pp. 2639–2643, 2012.

[13] P. Tabuada, "Event-triggered real-time scheduling of stabilizing control tasks," *IEEE Transactions on Automatic Control*, vol. 52, no. 9, pp. 1680–1685, 2007.

[14] D. V. Dimarogonas, E. Frazzoli, and K. H. Johansson, "Distributed event-triggered control for multi-agent systems," *IEEE Transactions on Automatic Control*, vol. 57, no. 5, pp. 1291–1297, 2012.

[15] G. S. Seybotha, D. V. Dimarogonas, and K. H. Johansson, "Event-based broadcasting for multi-agent average consensus," *Automatica*, vol. 49, no. 1, pp. 245–252, 2013.

[16] W. Zhu, Z. P. Jiang, and G. Feng, "Event-based consensus of multi-Agent systems with general linear models," *Automatica*, vol. 50, no. 2, pp. 552–558, 2014.

[17] H. Li, X. Liao, T. Huang, and W. Zhu, "Event-triggering sampling based leader-following consensus in second-order multi-agent systems," *IEEE Transactions on Automatic Control*, vol. 60, no. 7, pp. 1998–2003, 2015.

[18] Z. Chen, B. Niu, L. Zhang, J. F. Zhao, A. M. Ahmad, and M. O. Alassafi, "Command filtering-based adaptive neural network controlfor uncertain switched nonlinear systems using event-triggered communication," *International Journal of Robust and Nonlinear Control*, vol. 32, no. 11, pp. 6507–6522, 2022.

[19] Z. M. Li, X. H. Chang, and J. H. Park, "Quantized static output feedback fuzzy tracking control for discrete-time nonlinear networked systems with asynchronous event-triggered constraints," *IEEE Transactions on Systems, Man, and Cybernetics: Systems*, vol. 51, no. 6, pp. 3820–3831, 2021.

[20] Y. M. Zhou and X. H. Chang, "Event-triggered quantized L2−L∞$$ {\mathfrak{L}}_2-{\mathfrak{L}}_{\infty } $$ filtering for neural networks under denial-of-service attacks," *International Journal of Robust and Nonlinear Control*, vol. 32, no. 10, pp. 5897–5918, 2022.

[21] H. Su, M. Z. O. Chen, J. Lam, and Z. Lin, "Semi-global leader-following consensus of linear multi-agent systems with input

saturation via low gain feedback," *IEEE Transactions on Circuits and Systems I: Regular Papers*, vol. 60, no. 7, pp. 1881–1889, 2013.

[22] W. Qin, Z. Liu, and Z. Chen, "A novel observer-based formation for nonlinear multi-agent systems with time delay and intermittent communication," *Nonlinear Dynamics*, vol. 79, no. 3, pp. 1651–1664, 2015.

[23] Y. Hong, J. Hu, and L. Gao, "Tracking control for multi-agent consensus with an active leader and variable topology," *Automatica*, vol. 42, no. 7, pp. 1177–1182, 2006.

[24] W. Ren, R. W. Beardr, and E. M. Atkins, "Information consensus in multivehicle cooperative control," *IEEE Control Systems Magazine*, vol. 27, no. 2, pp. 71–82, 2007.

[25] P. Howlett, "An optimal strategy for the control of a train," *The Journal of the Australian Mathematical Society. Series B. Applied Mathematics*, vol. 31, no. 4, pp. 454–471, 1990.

[26] Y. Fu, *Research on Modeling and Simulations of Train Tracking Operation and Saving Energy Optimization*, Beijing Jiaotong University, China, 2009.

[27] S. Tarbouriech, G. Garcia, J. M. G. Silva, and I. Queinnec, *Stability and Stabilization of Linear Systems with Saturating Actuators*, Springer, London, 2011.

[28] M. C. Valentino, F. A. Faria, V. A. Oliveira, and L. F. C. Alberto, "Sufficient conditions in terms of linear matrix inequalities for guaranteed ultimately boundedness of solutions of switched Takagi-Sugeno fuzzy systems using the S-procedure," *Information Sciences*, vol. 572, no. 4, pp. 501–521, 2021.